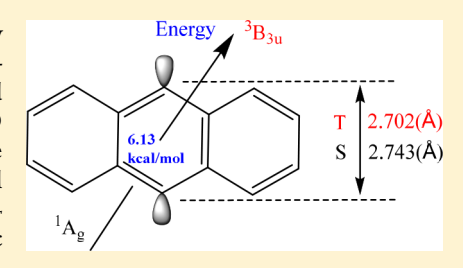
An Extended Multireference Study of the Singlet and Triplet States of the 9,10-didehydroanthracene Diradical

Hui Hu, Boyi Zhang, Adam Luxon, Thais Scott, Baoshan Wang, and Carol A. Parish*,

Department of Chemistry, Gottwald Center for the Sciences, University of Richmond, Richmond, Virginia 23173, United States [‡]College of Chemistry and Molecular Sciences, Wuhan University, Wuhan, Hubei Province 430072, P.R. China

Supporting Information

ABSTRACT: The 9,10-didehydroanthracene is an aromatic diradical produced by the Bergman cyclization of a benzannulated 10-membered enediyne. It is a 1,4 diradical, similar to p-benzyne. Here we study the spin state occupancy of the ground state of 9,10-didehydroanthracene by employing multireference methods (MR-CISD and MR-AQCC) with different basis sets (cc-pVDZ and cc-pVTZ) and active space sizes (CAS (2,2) through CAS (8,8)). At the CAS (8,8) MR-AQCC/cc-pVDZ level of theory, we find a two-configurational singlet ground state with an adiabatic $\Delta E_{\rm ST}$ of 6.13 kcal/mol. Unpaired electron density populations and dominant electronic configuration interactions were used to analyze the features of the 9,10didehydroanthracene diradical.



■ INTRODUCTION

The Bergman cyclization is an important rearrangement reaction involving a reactive diradical intermediate that plays a key role in cleaving DNA of antitumor drugs such as calicheamicin and dynemicin. Naturally occurring antitumor molecules such as calicheamicin undergo the Bergman cyclizaton reaction to produce p-benzyne, motivating interest in these molecules for their potential use in cancer treatments.^{2–27} Recently, Schuler et al.²⁸ characterized a reversible Bergman cyclization of a strained cyclic diyne (Figure 1). Using

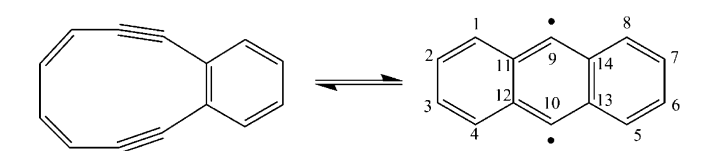


Figure 1. Bergman cyclization of the cyclic diyne 3,4-benzocyclodeca-3,7,9-triene-1,5-diyne.

atomic force microscopy (AFM), they were able to, for the first time, visualize and manipulate the resulting 9,10-didehydroanthracene diradical stabilized on a NaCl substrate surface. Using atomic manipulation, they reversibly induced retro-Bergman ring-opening as well as diradical reformation. The 9,10didehydroanthracene diradical, also known as the anthracene diradical, is a good model for the diradicals that form from the Bergman cyclization of natural product enediynes because of the size of the molecular system and the aromatic rings that bracket and conjugate with the middle diradical-containing ring. This molecule is closely related to p-benzyne, which has been the subject of many experimental and computational studies due its role as the intermediate of the simplest Bergman cyclization. Radical electron coupling between the dehydrocarbon atoms in p-benzyne leads to a stabilized singlet state which falls below the triplet state in energy. 29,30 To the best of our knowledge, there are no previous reports exploring these interactions in the anthracene diradical using highly correlated, multireference methods.

In general, diradicals are difficult to characterize computationally because of their multireference character. The openshell nature and relatively high electron count of 9,10didehydroanthracene make it a particularly challenging molecule for theoretical characterization. There have only been a few previous studies, which use either density functional theory (DFT), single-reference methods, or multireference methods with perturbative inclusion of dynamical correlation. Schottelius and Chen studied the geometry and energy of the singlet state of 9,10-didehydroanthracene using the multideterminantal CASPT2N method with (2,2), (4,4), and (6,6) active spaces and a 6-31G* basis set.⁶² The (4,4) and (6,6) active spaces included any σ and σ^* orbitals necessary to probe 1,4-diradical through-bond coupling and did not include any π orbitals. Zahradnik et al. calculated the heat of formation and ionization potential of the anthracene diradical using the semiempirical AM1 method.⁶³ Jones and Warner reported a singlet-triplet (ST) energy gap ($\Delta E_{ST} = E(\text{triplet})$ – E(singlet) = 5.2 kcal/mol) using an unrestricted DFT method (UBLYP/6-311+G**).64 Kim et al. used the spin-polarized Perdew-Burke-Ernzerhof (PBE) functional to study the singlet and triplet geometries and the adiabatic ST energy gap (4.2 kcal/mol). 65 The two aforementioned DFT studies predicted a singlet ground state for the 9,10-didehydroanthracene diradical. However, the study published most recently

Received: February 4, 2018 Revised: March 19, 2018 Published: March 20, 2018

Α

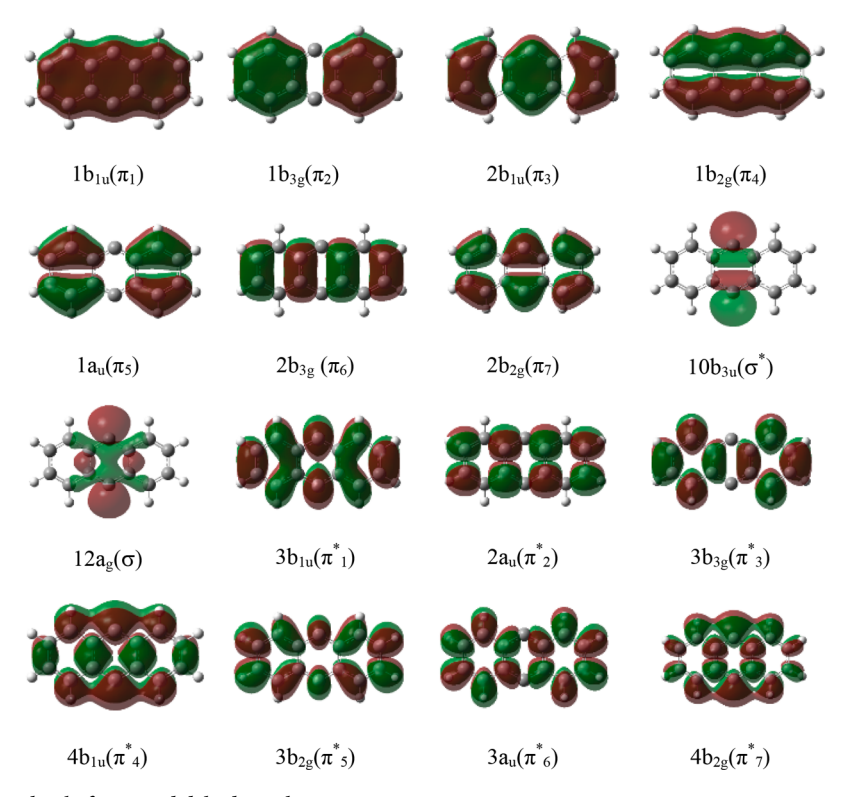


Figure 2. ROHF/cc-pVDZ orbitals for 9,10-didehydroanthracene.

by Schuler et al. predicted a triplet ground state using DFT with the PBE exchange-correlation functional.²⁸

Although DFT methods have been able to characterize diradicals with relative success in some cases, we cannot evaluate its ability to accurately capture the multiconfigurational nature of these systems. ⁶⁰ In the absence of an experimental analysis of the ST energy gap, it is difficult to know which of the predictions described above regarding the ground state spin multiplicity is correct. Highly correlated multireference (MR) methods, in contrast, can properly characterize the electronic interactions of diradicals and should give the most trustworthy answer as to which spin state is the ground state of 9,10-didehydroanthracene.

MR methods use a multiconfigurational wave function as a reference space to describe static correlation. The most common way to obtain a multireference wave function is through the complete active space self-consistent field (CASSCF) approach. Post-CASSCF approaches to treat dynamical correlation include multireference configurational interaction with single and double excitations (MR-CISD). Another is the multireference averaged quadratic coupled cluster (MR-AQCC) method, which inherently accounts for size-extensivity and is state-specific, characterizing each electronic state individually.

In this work, we present an application of the aforementioned highly correlated multireference methods to the characterization of the lowest lying singlet and triplet states of the 9,10-didehydroanthracene diradical. Various active space sizes were explored in order to understand the methodological dependence of the results. Properties such as important geometric parameters, orbital energies, unpaired electron densities, and Mulliken populations were analyzed to gain insight into the electronic structure and relative stability of the singlet and triplet states of the 9,10-didehydroanthracene diradical.

COMPUTATIONAL DETAILS

Initially, the triplet state of the anthracene diradical was geometry optimized using restricted open-shell Hartree–Fock (ROHF) with a cc-pVDZ basis set⁶⁹ using the Gaussian 09 program.⁷⁰

The orbitals (Figure 2) were assigned irreducible representation labels under D_{2h} symmetry. Geometry optimizations were performed using the multiconfigurational self-consistent field (MCSCF) method with starting geometries from the ROHF/ cc-pVDZ results. The orbital space for the MCSCF calculations was divided into doubly occupied (DOCC) and complete active space (CAS) sections. The DOCC orbitals were constrained to be doubly occupied in all configuration state functions (CSFs) and all possible CSFs in the CAS were constructed based on a given state symmetry. Geometry optimizations and energy computations with both the MR-CISD and MR-AQCC methods were subsequently run using MCSCF optimized orbitals. Size-extensivity corrections were computed by means of the Pople method (MR-CISD+Q), which is comprised of several variants of the Davidson correction. 71,7

An ideal active space for the anthracene diradical would be CAS (16,16), which would include the $1-7\pi$ and $1-7\pi^*$ orbitals as well as the σ and σ^* orbitals on the two radical centers. However, with the inclusion of dynamical electron correlation, our computational resources limited the largest feasible active space to be CAS (8,8). In order to assess the validity of the chosen active space, we explored a variety of active spaces ranging from CAS (2,2) to CAS (14,10) (vida infra).

Calculations were performed on the two lowest lying singlet and triplet states. MCSCF, MR-CISD, and MR-AQCC computations were carried out using the COLUMBUS 7.0 program $^{73-75}$ with the atomic orbital integral package from

Table 1. Natural Orbital Populations from Various CAS (12,12) MCSCF Singlet Single Point Calculations with the cc-pVDZ Basis Set

			$5\pi + 5\pi$	$\tau^* + 2\sigma$				$6\pi + 6\pi^*$		
irrep	orbital	1	2	3	4	5	6	7	8	9
$4b_{2g}$	π^*_7	0.0046	0.0044				0.0148		0.0202	0.0228
$3a_u$	π^*_{6}		0.0051		0.0058	0.0337		0.0324	0.0212	
$3b_{2g}$	π^*_5	0.0547	0.0352	0.0545	0.0345	0.0716	0.0605	0.0717	0.0674	0.0708
$4b_{1u}$	π^*_4			0.0059		0.0715	0.0675	0.0710	0.0396	0.0672
$3b_{3g}$	π^*_3	0.0836		0.0840	0.0083	0.0970	0.0777	0.0950		0.0814
$2a_u$	π^*_2	0.0586	0.0719	0.0591	0.0692	0.1142	0.0891	0.1116	0.0790	0.1066
$3b_{1u}$	π^*_{1}	0.1106	0.1371	0.1094	0.1364	1.8872	1.9054	1.8890	1.9155	1.8886
$12a_g$	σ	0.7984	0.7618	0.7986	0.7613					
$10b_{3u}$	σ^*	1.2016	1.2382	1.2013	1.2388					
$2b_{2g}$	π_7	1.8950	1.8624	1.8942	1.8626	1.9211	1.9425	1.9212	1.9800	1.9332
$2b_{3g}$	π_6	1.9392	1.9329	1.9393	1.9315	1.9268	1.9337	1.9268	1.9382	1.9291
$1a_u$	π_5	1.9161	1.9932	1.9166		1.9350	1.9439	1.9344		1.9413
$1b_{2g}$	π_4	1.9948				1.9944	1.9874		1.9876	1.9950
$2b_{1u}$	π_3	1.9430	1.9634	1.9427	1.9622	1.9678	1.9862	1.9685	1.9808	1.9812
$1b_{3g}$	π_2		1.9945		1.9944	1.9798		1.9806	1.9817	1.9828
$1b_{1u}$	π_1			1.9944	1.9951		1.9913	1.9978	1.9889	

DALTON.⁷⁶ The energy convergence criteria for MCSCF and MRCI were 1.0E(-8) and 1.0E(-6), respectively. The Dunning all-electron correlation consistent cc-pVDZ and cc-pVTZ (with the d orbitals on H removed for tractability) basis sets^{69,77} were employed. Unpaired electron densities and Mulliken populations were generated using the COLUMBUS 7.0 program. The Visual Molecular Dynamics⁷⁸ program and MOLDEN⁷⁹ were used to visualize these plots. For comparison to single reference (SR) results, we also performed geometry optimizations using the CCSD(T) method⁸⁰ with the cc-pVDZ basis set as available in the MOLPRO program.⁸¹

RESULTS AND DISCUSSION

Active Space Optimization. The smallest active space used for describing the anthracene diradical included only the σ and σ^* orbitals (CAS (2,2); $10b_{3u}$ and $12a_e$; Figure 2). This minimum active space was employed to estimate the ST energy gap, and to compare the effects of different basis sets. We calculated the MCSCF, MR-CISD, MR-CISD+Q, and MR-AQCC adiabatic (Table S1) and vertical (Table S2) ST energy gaps using a CAS (2,2) reference wave function with the ccpVDZ and cc-pVTZ basis sets. MR-AQCC/cc-pVTZ results show the singlet state to lie lower than the triplet by 3.03 (adiabatic) and 3.82 (vertical) kcal/mol. The results using a ccpVDZ basis set are very close to those of cc-pVTZ. The largest difference between the two basis sets was 0.22 and 0.44 kcal/ mol, in the MR-AQCC calculation, for the adiabatic and vertical excitation energies, respectively. The geometry parameters corresponding to this level of theory are shown in Table S3. There is little change in bond distances and angles between the different basis sets at the CAS (2,2) level. For instance, bond distances for all directly bonded atom pairs in the singlet are only 0.010-0.017 Å shorter for TZ than for DZ. The C9-C10 nonbonded distance between the didehydrocarbon atoms in the singlet show the largest deviation. This interaction is 0.030 Å shorter with TZ than DZ. At the CAS (2,2) level, the geometries and relative energies of the anthracene diradical are nearly unaffected by the choice of basis set used. For computational tractability, we will use the cc-pVDZ basis set for all subsequent calculations.

It is necessary to select a proper minimal active space that is sufficient for describing the most essential part of the wave function. Choosing a CAS (16,16) active space which incorporates all σ , σ^* , π , and π^* orbitals was not possible due to computational limitations. In order to determine which orbitals were most likely to contribute to any possible multiconfigurational character, we ran MCSCF single point calculations with the largest possible MCSCF active space (CAS (12,12)) and systematically included various combinations of σ , σ^* , π , and π^* orbitals. We used the MCSCF natural orbital coefficients to assess the occupation of each orbital (Table 1). Orbitals that were either unoccupied or close to doubly occupied were considered less important for inclusion in the active space than orbitals with partial occupations. (Dynamical correlation between electrons in nonactive orbitals is still included via the electronic excitations in the CI and AQCC expansions.)

Using the natural orbital information we next chose different size active spaces, including CAS (2,2), CAS (4,4), CAS (6,6), CAS (8,8) and CAS (10,10) to calculate the adiabatic ST energy gap at the MCSCF level with the cc-pVDZ basis set (Table 2). The results show that the CAS (2,2) active space is insufficient for characterizing the anthracene diradical. For the triplet, this active space provides only one configuration and is therefore equivalent to an ROHF treatment.

We also explored the impact of active space choices under the influence of dynamical electron configuration by computing

Table 2. Adiabatic ST Energy Gaps for Different CAS Sizes at the MCSCF Level with the cc-pVDZ Basis Set^a

CAS sizes	$\mathop{\Delta E_{\rm ST}}\limits_{}$	active orbitals
(2,2)	0.43	$10b_{3w}(\sigma^*)$ $12a_g(\sigma)$
(4,4)	3.20	$2b_{2g}(\pi^7)$, $10b_{3w}$ $12a_{g'}$ $3b_{1u}(\pi^*_1)$
(6,6)	2.85	$2b_{3g}(\pi^6)$, $2b_{2g'}$ $10b_{3u'}$ $12a_{g'}$ $3b_{1u'}$ $2a_{u}(\pi^*_{2})$
(8,8)	4.38	$1a_{u}(\pi^{5}), 2b_{3g'}, 2b_{2g'}, 10b_{3u'}, 12a_{g'}, 3b_{1u'}, 2a_{u'}, 3b_{3g}(\pi^{*}_{3})$
(10,10)	4.27	$2b_{1u}(\pi^3)$, $1a_w$ $2b_{3g}$, $2b_{2g}$, $10b_{3w}$ $12a_g$, $3b_{1w}$ $2a_w$ $3b_{3g}$, $4b_{1u}(\pi^*_4)$

[&]quot;A positive $\Delta E_{\rm ST}$ (kcal/mol) indicates a singlet ground state for the anthracene diradical.

Table 3. Comparison of the Singlet and Triplet Total Energies and MCSCF, MR-CISD, MR-CISD+Q, and MR-AQCC Adiabatic and Vertical ST Energy Gaps Using the cc-pVDZ Basis Set and the CAS (4,4), (6,6) and (8,8) Active Spaces^a

CAS (4,4) MCSCF			. 1.()	1 . ()	1: 1 .: AF (1 1/ 1)	.: 1 A F b (1 1/ 1)
MR-CISD			singlet (au)	triplet (au)	adiabatic $\Delta E_{\rm ST}$ (Kcal/mol)	vertical $\Delta E_{\rm ST}^{\ \ b}$ (kcal/mol)
MR-CISD+Q -536.536136 -536.530035 3.83 MR-AQCC -536.544624 -536.537676 4.36 CAS (6,6) MCSCF -534.773474 -534.768936 2.85 MR-CISD -536.011731 -536.006547 3.25 MR-CISD+Q -536.543810 -536.537504 3.96 MR-AQCC -536.552143 -536.544944 4.52 CAS (8,8) MCSCF -534.780064 -534.773079 4.38 4.15 MR-CISD -536.017476 -536.010439 4.42 4.89 MR-CISD+Q -536.550293 -536.541737 5.37 6.41 MR-AQCC -536.560963 -536.551189 6.13 7.18 SR CCSD(T) -536.642087 -536.634832 4.55 DFT BLYP ⁶⁴ PBE ⁶⁵ 5.20 PBE ⁶⁵	CAS (4,4)	MCSCF	-534.754963	-534.749865	3.20	
MR-AQCC -536.544624 -536.537676 4.36 CAS (6,6) MCSCF -534.773474 -534.768936 2.85 MR-CISD -536.011731 -536.006547 3.25 MR-CISD+Q -536.543810 -536.537504 3.96 MR-AQCC -536.552143 -536.544944 4.52 CAS (8,8) MCSCF -534.780064 -534.773079 4.38 4.15 MR-CISD -536.017476 -536.010439 4.42 4.89 MR-CISD+Q -536.550293 -536.541737 5.37 6.41 MR-AQCC -536.560963 -536.551189 6.13 7.18 SR CCSD(T) -536.642087 -536.634832 4.55 DFT BLYP ⁶⁴ 5.20 PBE ⁶⁵ 4.24		MR-CISD	-535.998870	-535.993565	3.33	
CAS (6,6) MCSCF -534.773474 -534.768936 2.85 MR-CISD -536.011731 -536.006547 3.25 MR-CISD+Q -536.543810 -536.537504 3.96 MR-AQCC -536.552143 -536.544944 4.52 CAS (8,8) MCSCF -534.780064 -534.773079 4.38 4.15 MR-CISD -536.017476 -536.010439 4.42 4.89 MR-CISD+Q -536.550293 -536.541737 5.37 6.41 MR-AQCC -536.560963 -536.551189 6.13 7.18 SR CCSD(T) -536.642087 -536.634832 4.55 DFT BLYP ⁶⁴ PBE ⁶⁵ 5.20 PBE		MR-CISD+Q	-536.536136	-536.530035	3.83	
MR-CISD		MR-AQCC	-536.544624	-536.537676	4.36	
MR-CISD+Q -536.543810 -536.537504 3.96 MR-AQCC -536.552143 -536.544944 4.52 CAS (8,8) MCSCF -534.780064 -534.773079 4.38 4.15 MR-CISD -536.017476 -536.010439 4.42 4.89 MR-CISD+Q -536.550293 -536.541737 5.37 6.41 MR-AQCC -536.560963 -536.551189 6.13 7.18 SR CCSD(T) -536.642087 -536.634832 4.55 DFT BLYP ⁶⁴ 5.20 PBE ⁶⁵ 5.20	CAS (6,6)	MCSCF	-534.773474	-534.768936	2.85	
MR-AQCC -536.552143 -536.544944 4.52 CAS (8,8) MCSCF -534.780064 -534.773079 4.38 4.15 MR-CISD -536.017476 -536.010439 4.42 4.89 MR-CISD+Q -536.550293 -536.541737 5.37 6.41 MR-AQCC -536.560963 -536.551189 6.13 7.18 SR CCSD(T) -536.642087 -536.634832 4.55 DFT BLYP ⁶⁴ 5.20 PBE ⁶⁵ 5.20		MR-CISD	-536.011731	-536.006547	3.25	
CAS (8,8) MCSCF -534.780064 -534.773079 4.38 4.15 MR-CISD -536.017476 -536.010439 4.42 4.89 MR-CISD+Q -536.550293 -536.541737 5.37 6.41 MR-AQCC -536.560963 -536.551189 6.13 7.18 SR CCSD(T) -536.642087 -536.634832 4.55 DFT BLYP ⁶⁴ 5.20 PBE ⁶⁵ 5.20		MR-CISD+Q	-536.543810	-536.537504	3.96	
MR-CISD		MR-AQCC	-536.552143	-536.544944	4.52	
MR-CISD+Q -536.550293 -536.541737 5.37 6.41 MR-AQCC -536.560963 -536.551189 6.13 7.18 SR CCSD(T) -536.642087 -536.634832 4.55 DFT BLYP ⁶⁴ 5.20 PBE ⁶⁵ 4.24	CAS (8,8)	MCSCF	-534.780064	-534.773079	4.38	4.15
MR-AQCC -536.560963 -536.551189 6.13 7.18 SR CCSD(T) -536.642087 -536.634832 4.55 DFT BLYP ⁶⁴ 5.20 PBE ⁶⁵ 4.24		MR-CISD	-536.017476	-536.010439	4.42	4.89
SR CCSD(T) -536.642087 -536.634832 4.55 DFT BLYP ⁶⁴ 5.20 PBE ⁶⁵ 4.24		MR-CISD+Q	-536.550293	-536.541737	5.37	6.41
DFT BLYP ⁶⁴ 5.20 PBE ⁶⁵ 4.24		MR-AQCC	-536.560963	-536.551189	6.13	7.18
PBE ⁶⁵ 4.24	SR	CCSD(T)	-536.642087	-536.634832	4.55	
·	DFT	BLYP ⁶⁴			5.20	
PBE on NaCl ²⁸ -3.46		PBE ⁶⁵			4.24	
122 01 11401		PBE on NaCl ²⁸			-3.46	

[&]quot;Orbitals for each active space are shown in Table 2. A positive energy gap indicates a singlet ground state. "All single point absolute energies included in Table S6 (Supporting Information).

Table 4. Dominant Configurations in the MR-CISD and MR-AQCC Results for the Singlet and the Triplet States computed Using the CAS (4,4), (6,6), and (8,8) Active Spaces with the cc-pVDZ Basis Set

76% 44% 71% 44%	$\% \ \pi_7^2(\sigma^*)^2 + 27\% \ \pi_7^2\sigma^2$ $\% \ \pi_7^2\sigma^1(\sigma^*)^1$ $\% \ \pi_6^2\pi_7^2(\sigma^*)^2 + 26\% \ \pi_6^2\pi_7^2\sigma^2$ $\% \ \pi_6^2\pi_7^2\sigma^1(\sigma^*)^1$ $\% \ \pi_5^2\pi_6^2\pi_7^2(\sigma^*)^2 + 26\% \ \pi_5^2\pi_6^2\pi_7^2(\sigma^*)^2$	$\pi_{-}G^2$	53% 34% 52%	$\pi_6^2 \pi_7^2 \sigma^1 (\sigma^*)^1$	$+17\% \ \pi_6^2 \pi_7^2 \sigma^2$
44% 71% 44%	$\% \ \pi_6^2 \pi_7^2 (\sigma^*)^2 + 26\% \ \pi_6^2 \pi_7^2 \sigma^2$ $\% \ \pi_6^2 \pi_7^2 \sigma^1 (\sigma^*)^1$	π - σ^2	34% 52%	$\pi_6^2 \pi_7^2 (\sigma^*)^2 + \pi_6^2 \pi_7^2 \sigma^1 (\sigma^*)^1$	1
71% 44%	$\% \pi_6^2 \pi_7^2 \sigma^1(\sigma^*)^1$	π - σ^2	52%	$\pi_6^2 \pi_7^2 \sigma^1 (\sigma^*)^1$	1
44%	0 / (/	π - σ^2		0 , , ,	
	$\% \pi_5^2 \pi_6^2 \pi_7^2 (\sigma^*)^2 + 26\% \pi_5^2 \pi_6^2 \pi_6^2$	π - σ^2	2.40/	2 2 2 4	
	3 0 7 0 7	10,0	$34\% \ \pi_5^2 \pi_6^2 \pi_7^2 (\sigma^*)^2 + 16\% \ \pi_5^2 \pi_6^2 \pi_7^2 \sigma^2$		
71%	$\% \pi_5^2 \pi_6^2 \pi_7^2 \sigma^1(\sigma^*)^1$		51%	$\pi_5^2 \pi_6^2 \pi_7^2 \sigma^1 (\sigma$	r*) ¹
(H8)	MCSCF/cc-pVDZ				(H8)
	(H8)	MR-CISD/cc-pVDZ	MR-CISD/cc-pVDZ 1.081 (1)		MR-CISD/cc-pVDZ 1.081

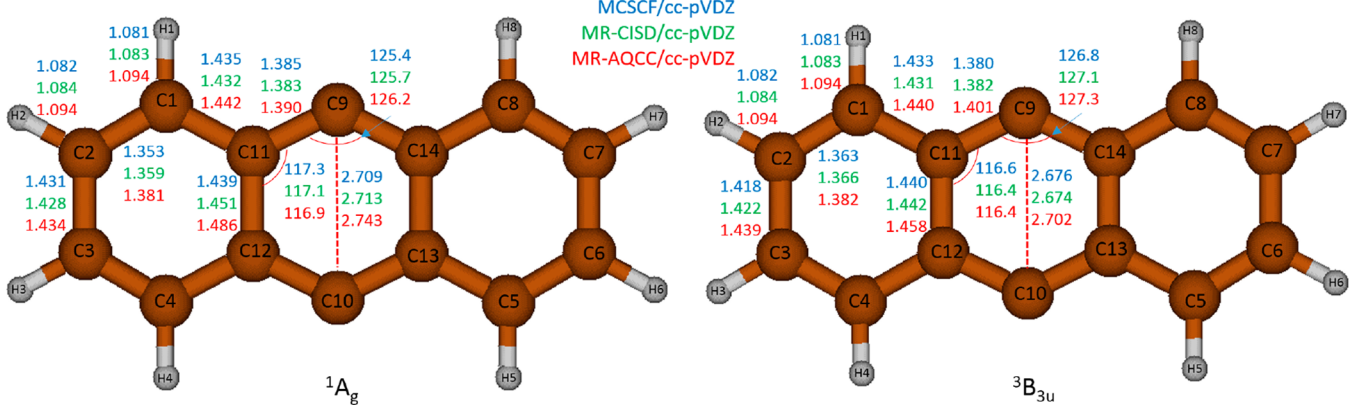


Figure 3. CAS (8,8) cc-pVDZ optimized geometries for 9,10 didehydroanthracene in the lowest singlet and triplet states. Values shown for MCSCF (blue), MR-CISD (green), and AQCC (red). The numbers denote the bond distance (Å) and bond angle (deg).

MR-CISD, MR-CISD+Q, and MR-AQCC adiabatic ST energy gaps for CAS (4,4), CAS (6,6), and CAS (8,8) reference wave functions with the cc-pVDZ basis set. The absolute and relative energies of the singlet and triplet states are shown in Table 3. This is an important test as interactions between electrons not included in the active space will be included as part of the dynamical correlation. From these results we determined that the CAS (8,8) active space provided the best balance of nondynamical electron correlation and computational tractability. The convergence with respect to adiabatic and vertical ST energy gap at CAS (8,8), along with the MCSCF natural

orbital information, suggested that the most important orbitals for inclusion in the active space were $1a_u(\pi_5)$, $2b_{3g}(\pi_6)$, $2b_{2g}(\pi_7)$, $10b_{3u}(\sigma^*)$, $12a_g(\sigma)$, $3b_{1u}(\pi^*_1)$, $2a_u(\pi^*_2)$, and $3b_{3g}(\pi^*_3)$. This active space was used to optimize the geometry of the lowest lying singlet and triplet state and to determine the corresponding adiabatic ST energy gap. In order to estimate vertical ST energy gaps, we also performed triplet state single point calculations using the MR-AQCC optimized singlet state geometry.

The Anthracene Diradical Has a Singlet Ground State. As shown in Table 3, the singlet state was found to be the

ground state at every theoretical level of our work. At the MCSCF/cc-pVDZ level of theory with a CAS (8,8) active space, the singlet lies 4.38 kcal/mol lower in energy than the triplet. The inclusion of electron correlation increases the ST energy gap by a small amount (4.42 and 5.37 kcal/mol for MR-CISD and MR-CISD+Q, respectively.) At the MR-AQCC level of theory, the singlet lies 6.13 kcal/mol lower in energy than the triplet (Table 3). We analyzed the dominant electronic configurations for the singlet and triplet states with CAS (4,4), (6,6), and (8,8) active spaces in MR-CISD and MR-AQCC computations with the cc-pVDZ basis set (Table 4). Configurations with weightings (square of the CSF coefficients) less than 10% were considered insignificant and are not reported. The singlet state (1Ag) is multireference with configurations $(\sigma^*)^2 \pi_5^2 \pi_6^2 \pi_7^2$ and $\sigma^2 \pi_5^2 \pi_6^2 \pi_7^2$ contributing 34% and 16%, respectively. The configuration state function with a doubly occupied out-of-phase σ^* orbital is the leading configuration in the singlet state, suggestive of through-bond coupling. 29,30 The 18% CSF weighting difference between $(\sigma^*)^2$ and σ^2 occupancy indicates that the σ^* orbital is lower in energy than the σ orbital, but that the gap between them is small enough to populate both levels. There is only one main configuration in the triplet state (3B311), namely a $\sigma^1(\sigma^*)^1\pi_5^2\pi_6^2\pi_7^2$ occupancy with a 51% weighting. Vertical ST energy gaps range from 4.15 kcal/mol at the MCSCF level, to 7.18 kcal/mol with MR-AQCC (Table 3).

Singlet and Triplet Geometries of the Anthracene Diradical are Similar. The CAS (8,8) AQCC/cc-pVDZ singlet and triplet geometries are remarkably similar in both of the outer aromatic rings, as well as in the middle ring containing the radical centers (Figure 3). The structural similarity between the two states suggests a lack of through space coupling between the dehydrocarbon atoms in the singlet, i.e. through-space coupling would lead to a large C9 — C10 orbital overlap and subsequent partial bond formation, which would distort the singlet geometry relative to the triplet geometry. The lack of through space coupling in the singlet is underscored by a C9—C10 distance that is 0.041 Å longer in the singlet than in the triplet at the AQCC level.

Electronic Structure of the Singlet and Triplet. We also examined the energies of the MCSCF optimized active space orbitals for the singlet and triplet states, both at the CAS (8,8) level of theory as well as for the CAS (2,2), (4,4), and (6,6) calculations (Table S7). With all active spaces, the out-of-phase $10b_{3u}$ (σ^*) orbital lies lower in energy than the $12a_g$ (σ) orbital, indicative of through-bond coupling between the electrons on the didehydrocarbon atoms. The σ and σ^* orbital energies in the singlet state are both negative (occupied) reflecting the increased two-configurational nature and the subsequent narrowing of the ST gap.

We calculated the Mulliken populations and unpaired electron densities (UED) for the singlet and triplet state at the CAS (8,8) AQCC/cc-pVDZ level (Figure 4). The UED and Mulliken analysis further underscores the similarity between the electronic structures of the singlet and triplet states. The Mulliken population in every atom is nearly the same for the two states. The biggest difference (0.025) is on the radical carbons. The total number of effective unpaired electrons is 2.126 for the singlet and 2.675 for triplet. This difference also comes mainly from the radical carbons, which are assigned 0.644 and 0.907 unpaired electrons for the singlet and triplet states, respectively. The observation that the singlet state has less total UED is consistent with the above energetic

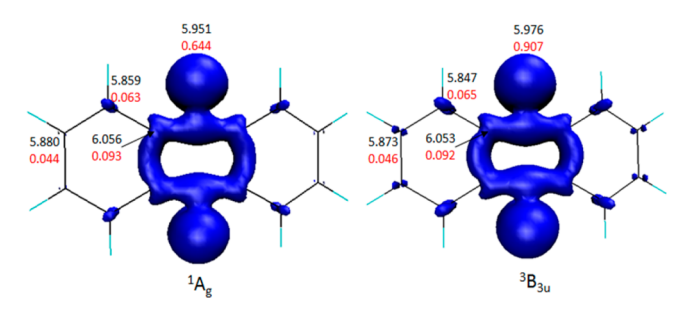


Figure 4. Unpaired electron density plot for the anthracene diradical (isovalue: 0.006). Also shown are unpaired electron populations (red) and Mulliken electron population (black) values. CAS (8,8) MR-AQCC/cc-pVDZ optimized geometries were used.

conclusion, and shows that radical interaction in the singlet state is a source of stabilization. Both energetics and UED indicate that the singlet state is the ground state for the anthracene diradical.

Comparison to p-Benzyne. The anthracene diradical is structurally similar to the well-studied p-benzyne diradical. Both species have singlet ground states with small adiabatic ST energy gaps (Table S8). The adiabatic ST energy gap in the anthracene diradical is 0.02 kcal/mol smaller than in *p*-benzyne at the MR-AQCC level.⁸² The anthracene and p-benzyne diradical have similar geometries, and for both diradicals, the ground state singlet and lowest lying triplet state have similar geometries (Figures 3 and S1) and electronic structures. The UED plots of the singlet and triplet p-benzyne are very similar to the anthracene diradical singlet and triplet UED images when compared with the same isovalue (Figure 4 and S2). The unpaired electron population on the radical carbons and total molecular UED in the anthracene diradical and para-benzyne are summarized in Table 5. In both molecules, the UED on the singlet didehydrocarbons is smaller than in the triplet, suggestive of electronic coupling. The smaller singlet-triplet difference in total UED for the anthracene diradical is likely due to the effect of delocalized electron density from conjugation with the neighboring acene rings.

Comparison to Previous Results. Previously, the energetics of the anthracene diradical have been studied using DFT methods. Most studies identified a singlet ground state, in agreement with our highly correlated MR results, and report small adiabatic ST energy gaps, ranging between 4 and 5 kcal/ mol (Table 4). Our highest level of theory (CAS (8,8) MR-AQCC) predicts the singlet to be lower in energy than the triplet by 6.13 kcal/mol (adiabatic). Schuler et al.²⁸ reported a DFT-based triplet ground state for both the free anthracene diradical as well as when adsorbed to a NaCl/Cu(100) surface. They report a $\Delta E_{\rm ST}$ of 3.46 kcal/mol in favor of the triplet on the NaCl/Cu(100)surface using the PBE exchange-correlation functional. In their work, the surface distorts the anthracene diradical to a nonplanar geometry, with the outer benzene rings bending toward the surface. This suggests that the surface may be playing a role in stabilizing the triplet. They do not report a geometry or a $\Delta E_{\rm ST}$ for the free diradical; however, the latter value can be estimated to be less than 1 kcal/mol from Figure 4e of the Schuler et al. report, with the triplet lying lower. ²⁸ It is important to note that Schuler et al.²⁸ generated a potential energy surface by driving the C-C distance of the bond formed during cyclization; it is not clear if the singlet and triplet geometries were fully optimized.

Table 5. Comparison of the Unpaired Electron Populations on the Didehydrocarbons and Total Molecular Unpaired Electron Density (UED) in the Anthracene and p-Benzyne Diradicals for the Singlet and Triplet States Using the CAS(8,8) AQCC/DZ Geometry and Wave Function

UED	Radical	Carbon	Total molecular		
CLD	Singlet	Triplet	Singlet	Triplet	
	0.644	0.907	2.126	2.675	
	0.567	0.864	1.489	2.103	

Table 6. Geometrical Parameters for the Anthracene Diradical Optimized with CAS (8,8) at the MR-AQCC/cc-pVDZ and CCSD(T)/cc-pVDZ Levels of Theory, in Comparison with the Geometries Obtained by Previous Calculations

	MR-A	MR-AQCC		CCSD(T)		BLYP ⁶⁴		PBE ⁶⁵	
	singlet	triplet	singlet	triplet	CASPT2N ⁶²	singlet	triplet	singlet	
d _{C9-C10} (Å)	2.743	2.702	2.760	2.705	2.70	2.737	2.691		
$d_{\text{C9-C11}}$ (Å)	1.390	1.401	1.395	1.403	1.37	1.378	1.394	1.38	
$d_{\rm C11-C12} \; ({\rm \AA})$	1.486	1.458	1.485	1.461	1.47	1.521	1.477	1.50	
∠C11−C9−C14 (deg)	126.2	127.3	125.6	127.4		127.6	128.4	127.8	

Previously, studies of the geometry of the anthracene diradical used DFT methods, and also the CASPT2N multireference method. The DFT geometries are in good agreement with our MR results (Table 6), suggesting that for this molecular system, geometries may not be dependent upon a MR treatment. This may be due to the geometric similarities between the singlet and triplet state (*vida supra*).

For instance, a comparison of the BLYP to MR-AQCC geometries shows that the C9–C10 radical electron distances in the triplet are a bit shorter than in the singlet (BLYP (Δ = 0.046 Å) and AQCC (Δ = 0.041 Å)). The C11–C12 distances are similar for all cases; however, the C9–C11 distances are elongated in the singlet and shortened in the triplet, similar to the singlet—triplet geometric changes found in *p*-benzyne. The angle that includes the dehydrocarbon radical (\angle C11–C9–C14) is smaller in the singlet state relative to the triplet state in both the MR-AQCC and BLYP results.

To better compare both the energetics and geometries obtained with SR and MR methods, we also geometry optimized the singlet and triplet with CCSD(T)/cc-pVDZ. The singlet–triplet gaps as well as the geometries agree well with the MR-AQCC/cc-pVDZ results (Tables 3 and 6). Excepting the Schuler et al. 28 report, the general agreement between DFT, SR, and MR results suggests that the dynamical electron correlation included in the density functional and CCSD(T) models is accurately capturing both the non-dynamical and dynamical components of this diradical system.

CONCLUSIONS

We have demonstrated the singlet state of the anthracene diradical to be the ground state using a variety of highly correlated, multireference methods. Geometry optimization using these methods produces singlet and triplet state structures that are very similar to each other. The singlet state is two configurational with a weighting of 34% $(\sigma^*)^2\pi_5^2\pi_6^2\pi_7^2$ and 16% $\sigma^2\pi_5^2\pi_6^2\pi_7^2$. A comparison of the electronic structure of each state suggests that there is a bit less unpaired electron density in the singlet state relative to the triplet state. This indicates that while there is more interaction between the radicals in the singlet state it only produces a slight

stabilization, leading to a relatively small ST energy gap (adiabatic 6.13; vertical 7.18 kcal/mol, respectively, at the MR-AQCC/cc-pVDZ level). The agreement between the SR-CCSD(T) and the MR-AQCC results suggests that the second configuration in the two-configuration singlet is not playing a significant role in the geometry or energetics. In this diradical, the single reference result may be capturing all of the important correlation effects.

ASSOCIATED CONTENT

Supporting Information

The Supporting Information is available free of charge on the ACS Publications website at DOI: 10.1021/acs.jpca.8b01233.

The Supporting Information includes absolute energies and geometries obtained using CAS(2,2); orbital energies at the MCSCF/cc-pVDZ level in the singlet and triplet state of 9,10-didehydroanthracene diradical; single point results used to determine adiabatic $E_{\rm ST}$; and important energetic and geometric parameters for p-benzyne, where the latter information is included for comparison to the anthracene diradical (PDF)

AUTHOR INFORMATION

Corresponding Author

*(C.A.P.) E-mail: cparish@richmond.edu. Telephone: (804) 484-1548.

ORCID

Baoshan Wang: 0000-0003-3417-9283 Carol A. Parish: 0000-0003-2878-3070

Notes

The authors declare no competing financial interest.

ACKNOWLEDGMENTS

C.A.P. and H.H. acknowledge support from the Department of Energy (Grant DE-SC0001093) and NSF RUI (Grant CHE-1213271). C.A.P. acknowledges the donors of the Petroleum Research Fund, administered by the American Chemical Society. Computational resources were provided, in part, by

the MERCURY supercomputer consortium under NSF Grant CHE-1626238. A.L. acknowledges support from the Arnold and Mabel Beckman Foundation through receipt of a Beckman Scholars award. B.Z. and T.S. acknowledge support from the University of Richmond Arts and Sciences Undergraduate Research Committee.

REFERENCES

- (1) Hoffmann, R. Of What Use Enediynes. Am. Sci. 1993, 81, 324-
- (2) Edo, K.; Mizugaki, M.; Koide, Y.; Seto, H.; Furihata, K.; Otake, N.; Ishida, N. The Structure of Neocarzinostatin Chromophore Possessing a Novel bicyclo [7,3,0] Dodecadiyne System. Tetrahedron Lett. 1985, 26, 331-334.
- (3) Lee, M. D.; Dunne, T. S.; Siegel, M. M.; Chang, C. C.; Morton, G. O.; Borders, D. B. Calichemicins, A Novel Family of Antitumor Antibiotics 1. Chemistry and Partial Structure of Calichemicins. J. Am. Chem. Soc. 1987, 109, 3464-3466.
- (4) Golik, J.; Clardy, J.; Dubay, G.; Groenewold, G.; Kawaguchi, H.; Konishi, M.; Krishnan, B.; Ohkuma, H.; Saitoh, K.; Doyle, T. W. Esperamicins, a Novel Class of Potent Antitumor Antibiotics. 2. Structure of Esperamicin X. J. Am. Chem. Soc. 1987, 109, 3461-3462.
- (5) Konishi, M.; Ohkuma, H.; Matsumoto, K.; Tsuno, T.; Kamei, H.; Miyaki, T.; Oki, T.; Kawaguchi, H.; et al. Dynemicin A, a novel antibiotic with the anthraquinone and 1,5-diyn-3-ene subunit. J. Antibiot. 1989, 42, 1449-1452.
- (6) Kraka, E.; Cremer, D. Computer Design of Anticancer Drugs. A New Enediyne Warhead. J. Am. Chem. Soc. 2000, 122, 8245-8264.
- (7) Casazza, A. M.; Kelley, S. L. Enediyne Antibiotics as Antitumor Agents; Marcel Dekker, Inc.: New York, 1995.
- (8) Maeda, H.; Edo, K.; Ishida, N. Neocarzinostatin: The Past, Present, and Future of an Anticancer Drug; Springer: New York, 1997.
- (9) Nicolaou, K. C.; Dai, W.-M.; Wendeborn, S. V.; Smith, A. L.; Torisawa, Y.; Maligres, P.; Hwang, C.-K. Enediyne Compounds Equipped with Acid-, Base-, and Photo-Sensitive Triggering Devices. Chemical Simulation of the Dynemicin A Reaction Cascade. Angew. Chem., Int. Ed. Engl. 1991, 30, 1032-1036.
- (10) Maier, M. E. Design of Enediyne Prodrugs. Synlett 1995, 1995, 13-26.
- (11) Schreiner, P. R. Cyclic enediynes: relationship between ring size, alkyne carbon distance, and cyclization barrier. Chem. Commun. 1998, 483-484.
- (12) Schreiner, P. R.; Prall, M. Myers-Saito Versus C²-C⁶ "Schmittel") Cyclizations of Parent and Monocyclic Enyne-Allenes: Challenges to Chemistry and Computation. J. Am. Chem. Soc. 1999, 121, 8615-8627.
- (13) Schreiner, P. R.; Prall, M.; Lutz, V. Fulvenes from Enediynes: Regioselective Electrophilic Domino and Tandem Cyclizations of Enynes and Oligoynes. Angew. Chem., Int. Ed. 2003, 42, 5757-5760.
- (14) Cramer, C. J. Bergman, Aza-Bergman, and Protonated Aza-Bergman Cylizations and Intermediate 2,5-Arynes: Chemistry and Challenges to Computation. J. Am. Chem. Soc. 1998, 120, 6261-6269.
- (15) Cramer, C. J.; Squires, R. R. Quantum Chemical Characterization of the Cyclization of the Neocarzinostatin Chromophore to the 1,5-Didehydroindene Biradical. Org. Lett. 1999, 1, 215-218.
- (16) Koga, N.; Morokuma, K. Comparison of Biradical Formation Between Enediyne and Enyne-Allene. Ab Initio CASSCF and MRSDCI Study. J. Am. Chem. Soc. 1991, 113, 1907-1911.
- (17) Lindh, R.; Persson, B. J. Ab Initio Study of the Bergman Reaction: the Autoaromatization of Hex-3-ene-1,5-diyne. J. Am. Chem. Soc. 1994, 116, 4963-4969.
- (18) Lindh, R.; Ryde, U.; Schutz, M. On the Significance of the trigger reaction in the action of the calicheamicin anti-cancer drug. Theor. Chem. Acc. 1997, 97, 203-210.
- (19) Wenthold, P. G.; Lipton, M. A. A Density Functional Molecular Orbital Study of the C2-C7 and C2-C6 Cyclization Pathways of 1,2,4-Heptatrien-6-ynes. The Role of Benzannulation. J. Am. Chem. Soc. 2000, 122, 9265-9270.

- (20) Wierschke, S. G.; Nash, J. J.; Squires, R. R. A Multiconfigurational SCF and Correlation-Consistent CI Study of the Structures, Stabilities, and Singlet-Triplet Splittings of o-, m-, and p-Benzyne. J. Am. Chem. Soc. 1993, 115, 11958-11967.
- (21) Cramer, C. J.; Debbert, S. Heteroaromatic substitution in aromatic sigma biradicals: the six pyridynes. Chem. Phys. Lett. 1998, 287, 320-326.
- (22) Ando, T.; Ishii, M.; Kajiura, T.; Kameyama, T.; Miwa, K.; Sugiura, Y. A new non-protein enediyne antibiotic N1999A2: Unique enediyne chromophore similar to neocarzinostatin and DNA cleavage feature. Tetrahedron Lett. 1998, 39, 6495-6498.
- (23) Roger, C.; Grierson, D. S. Toward the construction of enediyne prodrug systems related to the ring expanded artifact produced upon isolation of maduropeptin chromophore. Tetrahedron Lett. 1998, 39,
- (24) Vuljanic, T.; Kihlberg, J.; Somfai, P. Diastereoselective synthesis of the monosaccharide kedarosamine and incorporation in an analogue of the enediyne kedarcidin chromophore. J. Org. Chem. 1998, 63, 279-
- (25) Galm, U. H.; Hager, M. H.; Van Lanen, S. G.; Ju, J.; Thorson, J. S.; Shen, B. Antitumor Antibiotics: Bleomycin, Enediynes, and Mitomycin. Chem. Rev. 2005, 105, 739-758.
- (26) Halcomb, R. L. In Enediyne Antibiotics as Antitumor Agents; Borders, D. B.; Doyle, T. W., Eds. Marcel Dekker, Inc.: New York,
- (27) Schreiner, P. R. Monocyclic Enediynes: Relationships between Ring Sizes, Alkyne Carbon Distances, Cyclization barriers, and Hydrogen Abstraction Reactions. Singlet - Triplet Separations of Methyl - Substituted p - benzynes. J. Am. Chem. Soc. 1998, 120, 4184-
- (28) Schuler, B.; Fatayer, S.; Mohn, F.; Moll, N.; Pavliček, N.; Meyer, G.; Peña, D.; Gross, L. Reversible Bergman cyclization by atomic manipulation. Nat. Chem. 2016, 8, 220.
- (29) Hoffmann, R. Interaction of Orbitals through space and through bonds. Acc. Chem. Res. 1971, 4, 1-9.
- (30) Hoffmann, R.; Imamura, A.; Hehre, W. Benzynes, dehydroconjugated molecules, and the interaction of orbitals separated by a number of intervening sigma bonds. J. Am. Chem. Soc. 1968, 90, 1499-
- (31) Borden, W. T. Diradicals; John Wiley and Sons: New York,
- (32) Wenthold, P. G.; Paulino, J. A.; Squires, R. R. The absolute heats of formation of o- m- and p-benzyne. J. Am. Chem. Soc. 1991, 113, 7414-7415.
- (33) Wenthold, P. G.; Squires, R. R. Biradical thermochemistry from collision-induced dissociation threshold energy measurements. Absolute heats of formation of ortho-, meta- and para-benzyne. J. Am. Chem. Soc. 1994, 116, 6401-6412.
- (34) Wenthold, P. G.; Squires, R. R.; Lineberger, W. C. Ultraviolet photoelectron spectroscopy of the o-, m-, and p-benzyne negative ions. Electron affinities and singlet-triplet splittings for o-, m-, and pbenzyne. J. Am. Chem. Soc. 1998, 120, 5279-5290.
- (35) Al-Saidi, W. A.; Umrigar, C. J. Fixed-node diffusion Monte Carlo study of the structures of m-benzyne. J. Chem. Phys. 2008, 128,
- (36) Chattopadhyay, S.; Chaudhuri, R. K.; Mahapatra, U. S. Studies on *m*-benzyne and phenol via improved virtual orbital-complete active space configuration interaction (IVO-CASCI) analytical gradient method. Chem. Phys. Lett. 2010, 491, 102-108.
- (37) Clark, A. E.; Davidson, E. R. Model Studies of Hydrogen Atom Addition and Abstraction Processes Involving ortho-, meta-, and para-Benzynes. J. Am. Chem. Soc. 2001, 123, 10691-10698.
- (38) Cramer, C. J.; Nash, J. J.; Squires, R. R. A reinvestigation of singlet benzyne thermochemistry predicted by CASPT2 coupledcluster and density functional calculations. Chem. Phys. Lett. 1997, 277, 311-320.
- (39) Debbert, S.; Cramer, C. J. Systematic comparison of the benzynes, pyridynes, and pyridynium cations and characterization of

- the Bergman cyclization of Z-but-1-en-3-yn-1-yl isonitrile to the meta diradical 2,4-pyridyne. *Int. J. Mass Spectrom.* **2000**, 201, 1–15.
- (40) Evangelista, F. A.; Allen, W. D.; Schaefer, H. F. Coupling term derivation and general implementation of state-specific multireference coupled cluster theories. *J. Chem. Phys.* **2007**, *127*, 024102.
- (41) Evangelista, F. A.; Hanauer, M.; Kohn, A.; Gauss, J. A sequential transformation approach to the internally contracted multireference coupled cluster method. *J. Chem. Phys.* **2012**, *136*, 204108.
- (42) Evangelista, F. A.; Simmonett, A. C.; Schaefer, H. F., III; Mukherjee, D.; Allen, W. D. A companion perturbation theory for state-specific multireference coupled cluster methods. *Phys. Chem. Chem. Phys.* **2009**, *11*, 4728–4741.
- (43) Gao, J.; Jankiewicz, B. J.; Reece, J.; Sheng, H.; Cramer, C. J.; Nash, J. J.; Kenttamaa, H. I. On the factors that control the reactivity of *meta*-benzynes. *Chem. Sci.* **2014**, *5*, 2205.
- (44) Groner, P.; Kukolich, S. G. Equilibrium structure of gas phase obenzyne. J. Mol. Struct. 2006, 780–781, 178–181.
- (45) Hanauer, M.; Köhn, A. Pilot applications of internally contracted multireference coupled cluster theory, and how to choose the cluster operator properly. *J. Chem. Phys.* **2011**, *134*, 204111.
- (46) Jagau, T. C.; Prochnow, E.; Evangelista, F. A.; Gauss, J. Analytic gradients for Mukherjee's multireference coupled-cluster method using two-configurational self-consistent-field orbitals. *J. Chem. Phys.* **2010**, 132, 144110.
- (47) Kraka, E.; Anglada, J.; Hjerpe, A.; Filatov, M.; Cremer, D. *m*-Benzyne and bicyclo[3.1.0]hexatriene- which isomer is more stable? a quantum chemical investigation. *Chem. Phys. Lett.* **2001**, 348, 115—125.
- (48) Kraka, E.; Cremer, D. Ortho-, meta-, and para-benzyne. A comparative CCSD(T) investigation. *Chem. Phys. Lett.* **1993**, *216*, 333–340.
- (49) Kraka, E.; Cremer, D. CCSD(T) Investigation of the Bergman Cyclization of Enediyne. Relative Stability of o-, m-, and p-Didehydrobenzene. *J. Am. Chem. Soc.* **1994**, *116*, 4929–4936.
- (50) Lindh, R.; Lee, T. J.; Bernhardsson, A.; Persson, B. J.; Karlstrom, G. Extended ab Initio and Theoretical Thermodynamics Studies of the Bergman Reaction and the Energy Splitting of the Singlet o-, m-, and p-Benzynes. *J. Am. Chem. Soc.* **1995**, *117*, 7186–7194.
- (51) Logan, C. F.; Chen, P. Ab Initio Calculation of Hydrogen Abtraction Reactions of Phenyl Radical and p-Benzyne. J. Am. Chem. Soc. 1996, 118, 2113–2114.
- (52) Melin, J.; Fuentealba, P. Application of the Electron Localization Function to Radical Systems. *Int. J. Quantum Chem.* **2003**, 92, 381–390.
- (53) Mullinax, J. W.; Sokolov, A. Y.; Schaefer, H. F. Can Density Cumulant Function Theory Describe Static Correlation Effects? *J. Chem. Theory Comput.* **2015**, *11*, 2487–2495.
- (54) Newton, M. D.; Fraenkel, H. A. The equilibrium geometry, electronic structure, and heat formation of ortho-benzyne. *Chem. Phys. Lett.* **1973**, *18*, 244.
- (55) Noell, J. O.; Newton, M. D. Equilibrium geometries and relative energies of the lowest singlet and triplet states of *o-,m-*, and *p-*Benzyne. *J. Am. Chem. Soc.* **1979**, *101*, 51.
- (56) Rinkevicius, Z.; Agren, H. Spin-flip time dependent density functional theory for singlet-triplet splittings in σ - σ -biradicals. *Chem. Phys. Lett.* **2010**, *491*, 132–135.
- (57) Rivero, P.; Jimenez-Hoyos, C. A.; Scuseria, G. E. Predicting Singlet-Triplet Energy Splittings with Projected Hartree-Fock Methods. *J. Phys. Chem. A* **2013**, *117*, 8073–8080.
- (58) Scheiner, A. C.; Schaefer, H. F.; Liu, B. J. Am. Chem. Soc. 1989, 111, 3118–3124.
- (59) Slipchenko, L. V.; Krylov, A. I. Singlet-triplet gaps in diradicals by the spin-flip approach: A benchmark study. *J. Chem. Phys.* **2002**, 117, 4694–4708.
- (60) Wang, E. B.; Parish, C. A.; Lischka, H. An extended multireference study of the electronic states of para-benzyne. *J. Chem. Phys.* **2008**, *129*, 044306.

- (61) Crawford, T. D.; Kraka, E.; Stanton, J. F.; Cremer, D. Problematic p-benzyne: Orbital instabilities, biradical character, and broken symmetry. *J. Chem. Phys.* **2001**, *114*, 10638–10650.
- (62) Schottelius, M. J.; Chen, P. 9,10-Dehydroanthracene: p-Benzyne-Type Biradicals Abstract Hydrogen Unusually Slowly. *J. Am. Chem. Soc.* **1996**, *118*, 4896–4903.
- (63) Zahradnik, R.; Hobza, P.; Burcl, R.; Hess, B. A. Strained Unsaturated Molecules Theoretical-Study of Acyclic and Cyclic Cumulenes and Acetylenes. *J. Mol. Struct.: THEOCHEM* **1994**, *313*, 335–349
- (64) Jones, G. B.; Warner, P. M. Electronic Control of the Bergman Cyclization: The Remarkable Role of Vinyl Substitution. *J. Am. Chem. Soc.* **2001**, *123*, 2134–2145.
- (65) Kim, H.-J.; Wang, X.; Ma, J.; Cho, J.-H. A density-functional-theory study of biradicals from benzene to hexacene. *Chem. Phys. Lett.* **2011**, *516*, 141–145.
- (66) Lischka, H.; Dallos, M.; Shepard, R. Analytic MRCI gradient for excited states: formalism and application to the n-pi* valence- and n-(3s,3p) Rydberg states of formaldehyde. *Mol. Phys.* **2002**, *100*, 1647–1658.
- (67) Szalay, P. G.; Bartlett, R. J. Multireference Averaged Quadratic Coupled-Cluster Method a Size-Extensive Modification of Multireference CI. *Chem. Phys. Lett.* **1993**, *214*, 481–488.
- (68) Szalay, P. G.; Muller, T.; Lischka, H. Excitation energies and transition moments by the multireference averaged quadratic coupled cluster (MR-AQCC) method. *Phys. Chem. Chem. Phys.* **2000**, *2*, 2067–2073.
- (69) Dunning, T. H., Jr Gaussian basis sets for use in correlated molecular calculations. I. The atoms boron through neon and hydrogen. *J. Chem. Phys.* **1989**, *90*, 1007–1023.
- (70) Frisch, M. J.; Trucks, G. W.; Schlegel, H. B.; Scuseria, G. E.; Robb, M. A.; Cheeseman, J. R.; Scalmani, G.; Barone, V.; Petersson, G. A.; Nakatsuji, H.; et al.. *Gaussian 09*, revision D.01; Gaussian, Inc.: Wallingford, CT, 2016.
- (71) Davidson, E. R. The World of Quantum Chemistry; Reidel: Dordrecht, The Netherlands, 1974.
- (72) Duch, W.; Diercksen, G. H. F. Size-extensivity corrections in configuration interaction methods. *J. Chem. Phys.* **1994**, *101*, 3018–3030.
- (73) Lischka, H.; Shepard, R.; Pitzer, R. M.; Shavitt, I.; Dallos, M.; Muller, T.; Szalay, P. G.; Seth, M.; Kedziora, G. S.; Yabushita, S.; et al. High-level multireference methods in the quantum-chemistry program system COLUMBUS: Analytic MR-CISD and MR-AQCC gradients and MR-AQCC-LRT for excited states, GUGA spin-orbit CI and parallel CI density. *Phys. Chem. Chem. Phys.* 2001, 3, 664–673.
- (74) Lischka, H.; Müller, T.; Szalay, P. G.; Shavitt, I.; Pitzer, R. M.; Shepard, R. Columbus—a program system for advanced multi-reference theory calculations. *Wiley Interdiscip. Rev. Comput. Mol. Sci.* **2011**. *1*. 191–199.
- (75) Lischka, H.; Shepard, R.; Shavitt, I.; Pitzer, R. M.; Dallos, M.; Müller, T.; Szalay, P. G.; Brown, F. B.; Ahlrichs, R.; Böhm, H. J.; Chang, A.; et al.. *COLUMBUS, an ab initio electronic structure program,* release 7.0, 2015.
- (76) Helgaker, T.; Jensen, H. J. A.; Jorgensen, P.; Olsen, J.; Ruud, K.; Agren, H.; Andersen, T.; Bak, K. L.; Bakken, V.; Christiansen, O., et al.. *DALTON, an ab initio electronic structure program,* Release 1.0., 1997.
- (77) Kendall, R. A.; Dunning, T. H., Jr.; Harrison, R. J. Electron Affinities of the First-Row Atoms Revisited: Systematic Basis Sets and Wave Functions. *J. Chem. Phys.* **1992**, *96*, 6796–6708.
- (78) Humphrey, W.; Dalke, A.; Schulten, K. VMD Visual Molecular Dynamics. *J. Mol. Graphics* **1996**, *14*, 33–38.
- (79) Schaftenaar, G.; Noordik, J. H. Molden: a pre- and post-processing program for molecular and electronic structures. *J. Comput. Aided Mol. Des.* **2000**, *14*, 123–134.
- (80) Watts, J. D.; Gauss, J.; Bartlett, R. J. Coupled-cluster methods with noniterative triple excitations for restricted open-shell Hartree–Fock and other general single determinant reference functions. Energies and analytical gradients. *J. Chem. Phys.* **1993**, *98*, 8718–8733.

- (81) Werner, H.-J.; Knowles, P. J.; Knizia, G.; Manby, F. R.; Schütz, M. Molpro: a general-purpose quantum chemistry program package. *Wiley Interdiscip. Rev. Comput. Mol. Sci.* **2012**, *2*, 242–253.
- (82) Zhang, B.; Annas, C.; Parker, A. J.; Mancini, J. S.; Wang, E. B.; Saldana Greco, D.; Nelson, E. S.; Springsted, G.; Parish, C. A.; Lischka, H., A Multireference Averaged Quadratic Coupled Cluster (MR-AQCC) Study of the Geometries and Energies for Ortho-, Meta- and Para-benzyne. Personal communication.